

# Autonomous Discovery of Unknown Reaction Pathways from Data by Chemical Reaction Neural Network

Weiqi Ji, Sili Deng

{weiqiji, silideng}@mit.edu

Department of Mechanical Engineering, Massachusetts Institute of Technology, MA 02139

## Abstract

The inference of chemical reaction networks is an important task in understanding the chemical processes in life sciences and environment. Yet, only a few reaction systems are well-understood due to a large number of important reaction pathways involved but still unknown. Revealing unknown reaction pathways is an important task for scientific discovery that takes decades and requires lots of expert knowledge. This work presents a neural network approach for discovering unknown reaction pathways from concentration time series data. The neural network denoted as Chemical Reaction Neural Network (CRNN), is designed to be equivalent to chemical reaction networks by following the fundamental physics laws of the Law of Mass Action and Arrhenius Law. The CRNN is physically interpretable, and its weights correspond to the reaction pathways and rate constants of the chemical reaction network. Then, inferring the reaction pathways and the rate constants are accomplished by training the equivalent CRNN via stochastic gradient descent. The approach precludes the need for expert knowledge in proposing candidate reactions, such that the inference is autonomous and applicable to new systems for which there is no existing empirical knowledge to propose reaction pathways. The physical interpretability also makes the CRNN not only capable of fitting the data for a given system but also developing knowledge of unknown pathways that could be generalized to similar chemical systems. Finally, the approach is applied to several chemical systems in chemical engineering and biochemistry to demonstrate its robustness and generality.

**Keywords:** Chemical Reaction Network; Chemical Reaction Neural Network; Physical Interpretable; Law of Mass Action; Stochastic Gradient Descent

## 1. Introduction

Identifying the chemical reaction network (CRN) behind the chemical process in biology, environment, and engineering is paramount to understanding the mechanism of disease, pollution, and manufacture. For example, the Mitogen-activated protein (MAP) kinases participated in signal transduction pathways control the intracellular events including acute responses to hormones and major developmental changes in organisms (1). Moreover, the

combustion chemistry (2) and atmosphere chemistry have enabled us to model and understand the formation and conversion of air pollutions.

The studies on CRN in physical chemistry have a long history after the discovery of the law of mass action. The development of CRN usually involves two steps: identification of the reaction pathways and determination of the rate constants. The CRN is usually developed by proposing reaction pathways based on expert knowledge and estimating the rate constants using computational chemistry and statistical inference from experimental data. However, there are still lots of important reaction pathways that are not identified yet, some of which would take us many decades to discover.

Meanwhile, with the increasing amount of sensor data and computational resources, there is increasing interest in the data-driven autonomous discovery of CRN. While various algorithms can robustly inference the rate constants from experimental data for given reaction network pathways (3, 4), even for large CRN with thousands of species and reaction pathways (5), it is still challenging to infer the reaction pathways from an infinite number of possible reactions. The infinity is due to that any two species can react with each other, and there could be multiple reaction pathways between two species.

On the other hand, high-throughput experiments have enabled us to run a series of batch reactors in parallel and measure a large amount of concentration time series data. Therefore, various approaches have been proposed to automatically discover reaction pathways from concentration time series data (6–12). Those approaches can be categorized into two branches: the expert-system-based and canonical-form-based approaches.

In the expert-system-based approach, a large number of possible reaction pathways are proposed based on expert knowledge, and then a compact model is determined via regularization following the principle of Occam's Razor. For example, the Reactive Sindy (11) approach employs  $L_1$  regularization to select important pathways. Automatic Reaction Mechanism Generator (RMG) (13) employs reaction flux analysis to identify important pathways. However, the approach is relied on a good initial guess based on expert knowledge, which precludes the application in a new reaction system with a lot of unknown reaction pathways. In addition, the initial proposal could be a huge system for complex reaction process. For example, current biology (14, 15) and combustion reaction systems (16) could contain more than  $10^4$  candidate reactions due to a large number of intermediate species. Then identifying a compact set of reactions from such a large system is computationally challenging.

In the canonical-form-based approaches, the underlying CRN is represented in a canonical form of power-law expressions. Then the reaction pathways, as well as the rate constants, are revealed via fitting the prediction of the canonical form with experimental data. Notably, the S-system (17–20), which is popular in the system biology community, could discover reaction pathways in a new reaction system without expert knowledge. The fitting is accomplished by optimizing a high-dimensional and nonlinear loss function which measures the fitness between model and time-dense species profile measurements. Various heuristic optimization approaches and mixed-

integer optimization approaches have been proposed for the optimization. However, it is still challenging to scale up the approach to large CRN with thousands of reactions.

This work is also motivated to autonomously discover reaction pathways from experimental measurements of concentration time series data. Especially for the chemical systems that we have limited knowledge of, which is challenging to propose reaction pathways for. For example, we still know little about the formation pathways of soot particles and soot precursors in flames (21), and it is challenging to explore the possible reaction pathways using Ab initio quantum chemistry for those complex precursors comprising a large number of atoms.

Our approach also takes the concept of canonical form, but instead represent the CRN using a neural network model and optimize it using stochastic gradient descent (SGD). The success of deep learning has shown that the optimization algorithm of SGD can effectively and robustly optimize large-scale nonlinear and non-convex network models (22). The rapid development of delicate computational hardware and open-source software platform (23, 24) for the deep neural network also enable the training of large-scale networks for various research communities. Inspired by the success of SGD in deep learning, we employ SGD to optimize the complex reaction network models. Furthermore, we shall show that the CRN can be represented in the form of a neural network with the weights of the neural network corresponding to the reaction formulas and the rate constants. Therefore, the neural network is physically interpretable and we call it Chemical Reaction Neural Network (CRNN). Then, the inference of reaction pathways and rate constants in CRN is accomplished by training the CRNN against the experimental data using SGD.

The physical interpretability makes the CRNN capable of not only fitting the data for a given system but also discovering unknown pathways. The newly discovered pathways, as a piece of abstract knowledge, can be transferred to similar systems. For example, the combustion chemistry model for large hydrocarbons is usually developed based on rate rules (25), i.e., the same rate constants can be applied to the same class of reactions with different reactants and products for different fuels. Such abstraction and generalization process is indeed the advantage of physics-based modelling comparing to black-box neural network modelling. The learned CRNN can also be converted to a standard format of CRN, which could be conveniently integrated into existing reactive flow solvers. The derivation of the physical interpretable neural network also provides a general approach for embedding fundamental physics laws into neural network models and contributes to the recent blooming of scientific machine learning (26).

Next, we shall first present the formula of CRNN and then apply it into three reaction systems ranging from chemical engineering to system biology. The code for the demonstrations is available upon request.

## 2. Chemical Reaction Neural Network (CRNN)

### 2.1 Derivation of Physically Interpretable CRNN

Without loss of generality, we derive the CRNN from classical CRN using the following single-step reaction involving four species of [A, B, C, D], and the stoichiometric coefficients of  $[v_A, v_B, v_C, v_D]$ .



Recall the Law of Mass Action discovered by Guldberg in 1879, the rates of (Eq. 1) can be expressed in the power-law expression with rate constant  $k$  and species concentration  $[A], [B]$ , shown in (Eq. 2). The expression can also be written as a cascade of exponential operation and linear weighted summation of species concentrations in the logarithmic scale, shown in (Eq. 3).

$$R = k[A]^{v_A}[B]^{v_B}[C]^{v_C}[D]^{v_D} \quad (\text{Eq. 2})$$

$$R = \exp(\ln k + v_A \ln[A] + v_B \ln[B] + v_C \ln[C] + v_D \ln[D]) \quad (\text{Eq. 3})$$

Together with the stoichiometric coefficients, the rates for each species can be represented by the following neuron, shown in Fig. 1. The inputs are the species concentrations in the logarithmic scale. The weights in the input layer correspond to the reaction orders, i.e.,  $[v_A, v_B, 0, 0]$  for [A, B, C, D], respectively. The species not presented in the reactants have the weights of zero. The bias corresponds to the rate constants in the logarithmic scale. The weights in the output layer correspond to the stoichiometric coefficients, i.e.,  $[-v_A, -v_B, v_C, v_D]$  for [A, B, C, D], respectively.

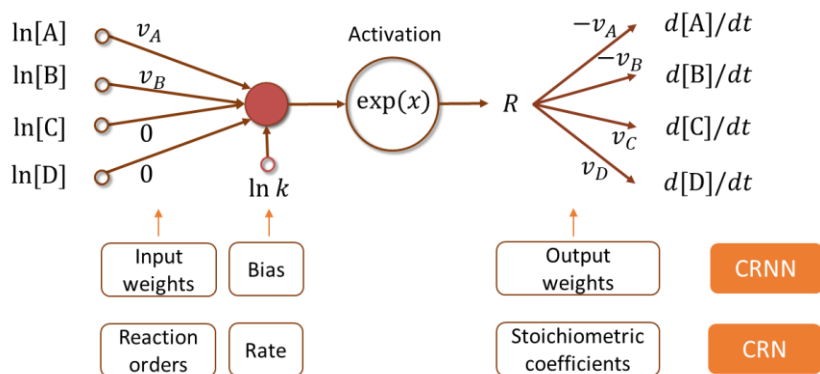


Fig. 1. A single neuron formulated with the Law of Mass Action for a single-step reaction. The annotations in the bottom present the equivalent components in the chemical reaction network (CRN) and chemical reaction neuron network (CRNN).

In many chemical reaction systems, the rate constants are changing with the environment. For example, the temperature dependence follows the Arrhenius Law discovered by Arrhenius in 1889. The modified three-parameters Arrhenius formula states that

$$k = AT^b \exp\left(-\frac{E_a}{RT}\right), \quad (\text{Eq. 3})$$

where  $A$  is the pre-factor or collision frequency factor,  $b$  is a fitting parameter to capture the non-exponential temperature dependence,  $E_a$  is the activation function, and  $R$  is the gas

constant. Equation 3 can also be written as a linear operation of temperature and the pre-factor  $A$  in (Eq. 4) and represented with the neuron shown in Fig. 2.

$$\ln k = \ln A + b \ln T - \frac{Ea}{RT} \quad (\text{Eq. 4})$$

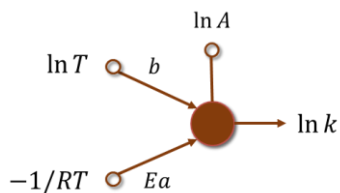


Fig. 2. A single neuron formulated with Arrhenius Law, which shows the dependence of the reaction rate constants on the temperature.

Combining the Law of Mass Action and Arrhenius Law, we could represent a single-step reaction of (Eq. 1) with a single neuron shown in Fig. 3. The weights and bias of the input layer correspond to the rate constants and the output layer tell the reaction formula. The activation function here is the exponential function.

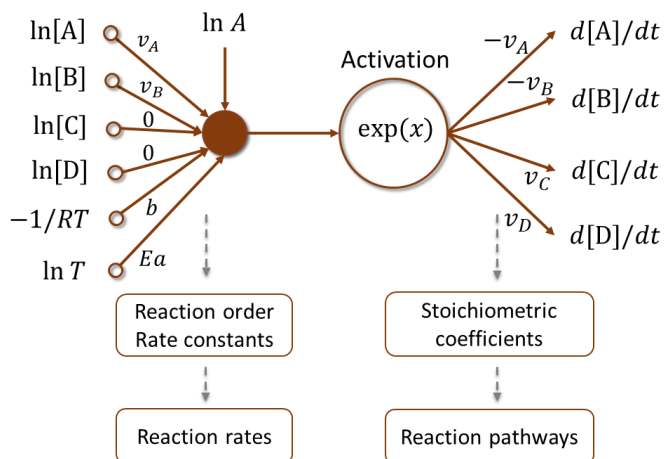


Fig. 3. A single neuron that represents a single-step reaction, following the Law of Mass Action and Arrhenius Law.

Beyond a single-step reaction, by stacking multiple neurons into one hidden layer, a neural network is then formulated to represent a multi-step reaction network comprising of  $m$ -species and  $n$ -reactions, as shown in Fig. 4. The species concentrations are denoted as  $[y_1, y_2, \dots, y_m]$ . The number of hidden nodes is equal to the number of reactions. We denote the neural network as Chemical Reaction Neuron Network (CRNN).

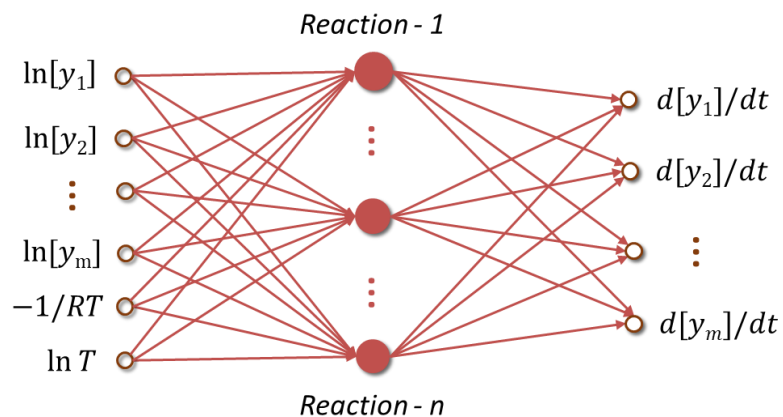


Fig. 4. A Chemical Reaction Neuron Network (CRNN) representing a multi-steps reaction network with the number of hidden nodes equal to the number of reactions.

## 2.2 Training of CRNN

Since the CRNN is equivalent to classical CRN, the inference of CRN then can be accomplished by training of CRNN. Considering a general form of a chemical reaction system that could be described by a CRN, the vector of species concentration  $\mathbf{Y}$  evolves with time according to

$$\dot{\mathbf{Y}} = \text{CRN}(\mathbf{Y}) \quad (\text{Eq. 5})$$

And we are trying to learn a CRNN that satisfies

$$\dot{\mathbf{Y}} = \text{CRNN}(\mathbf{Y}) \quad (\text{Eq. 6})$$

The CRNN can be trained from the data pair of  $\{\mathbf{Y}, \dot{\mathbf{Y}}\}$  collected at a different instance from different initial conditions. In practice, we are able to measure the concentration time series data, while it is challenging to measure the derivative directly. Various approaches have been developed for approximating derivative from noise data (27, 28). To illustrate the effectiveness of the representation, this work shall use synthesized data in which the derivative is exactly computed from the underlying CRN. Although, numerical tests show that the approach is robust to moderate level of noise in  $\mathbf{Y}$  and  $\dot{\mathbf{Y}}$ , the validation with noise suffers from the parameter identification difficulty for complex reaction network (3) that only important reaction pathways can be inferred with a limited amount of data. Nevertheless, the approach is expected to work for noise data, similar to the effectiveness of deep neural networks with SGD from noisy real-world data.

With the time-invariant concatenation data pair of  $\{\mathbf{Y}, \dot{\mathbf{Y}}\}$ , the loss function can be designed with the mean square error (MSE) as in (Eq. 7).

$$\text{Loss} = \text{MSE}(\text{CRNN}(\mathbf{Y}), \dot{\mathbf{Y}}^{data}) \quad (\text{Eq. 7})$$

The loss can be minimized with the popular SGD algorithm of Adam (29) using the recommended learning rate of 0.001.

With all of the species are known, the number of hidden nodes is the major hyperparameter to determine in order to determine the structure of CRNN. Here, we present two ‘regularization’ approaches to determine the number of hidden nodes, i.e., the number of proposed reactions. Both approaches will be illustrated in the case studies. The first one is ‘L<sub>0</sub> regularization’, i.e., penalty the number of hidden nodes. It can be accomplished via grid searching, i.e., increasing the number of proposed reactions until there is no gain of performance.

The second one is ‘L<sub>1</sub>+L<sub>2</sub> regularization’, following the concept of Sindy (30) and Reactive Sindy (11), i.e.,

$$\text{Loss} = \text{MSE}(\text{CRNN}(\mathbf{Y}), \dot{\mathbf{Y}}^{data}) + \alpha(\|\text{rate constants}\|_1 + \|\text{rate constants}\|_2) \quad (\text{Eq. 8})$$

The L<sub>2</sub> regularization is necessary to avoid the collinearity among reactions, i.e., a reaction could be written into two identical reactions with the rate constants halved. It is noted that the ‘L<sub>1</sub>+L<sub>2</sub> regularization’ implicitly assumes that all of the rate constants have the same weights. The assumption can be broken for large scale nonlinear CRN, and more advanced regularization based on reaction mechanism reduction, such as Direct Graph Theory (DRG) (31), can be applied on the fly.

### 3. Results

#### 3.1 Synthesis reactions network without temperature dependence

The first CRN is a hypothetical reaction network, taken from (32), comprising five chemical species labeled as  $x_1, \dots, x_5$  involved in four reactions with rate coefficients  $k_1 = 0.1, k_2 = 0.2, k_3 = 0.13, k_4 = 0.3$ , as shown in (Eq. 9). The case is chosen to assess the capability of CRNN in learning reaction pathways and illustrate the regularization algorithms. Thus, the temperature dependence of rate constants is not considered in this case.



The initial reactants are  $x_1$  and  $x_2$ . A total of 30 experiments are simulated in which the initial concentrations are randomly drawn from  $x_1 \in [0, 1], x_2 \in [0, 1]$ . In each case, the species concentrations and their temporal derivative were sampled every 0.1 time unit from 0 to 20 time units. Then totally, 6000 data pair is generated and divided into train and test datasets by 67% and 33%, respectively. To accelerate the training process, the weights of the input layer is forced to be non-negative, since the reaction order is usually non-negative. And the reaction order is

forced to be equal to the corresponding stoichiometric coefficient, which is held for non-catalytic reactions.

We first use the  $L_0$  regularization to determine the number of hidden nodes. Figure 5 shows the changes in training and test loss versus the number of hidden nodes. As expected, the loss decreases when the number of proposed reactions is less than four and reaches a plateau after that. It then can be inferred that the system kinetics could be well described using four reactions.

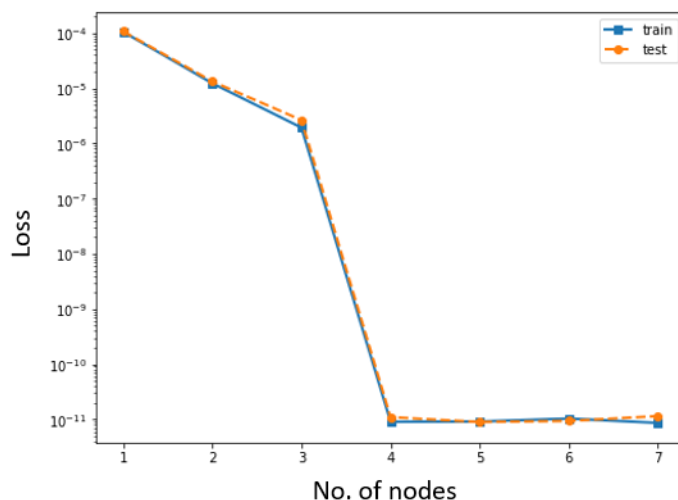


Fig. 5. The minimum training and test loss versus the number of hidden nodes in CRNN.

Figure 6 then shows the weights and bias of the trained CRNN with four hidden nodes. The heatmap can be read row by row, and each row corresponds to a reaction. The heatmap for the input weights reveals the reaction orders of each reaction. The heatmap for the output weights corresponds to the stoichiometric coefficients of each reaction. The heatmap for the bias corresponds to the rate constants of each reaction.

For example, from the first row of the heatmap for output weights, we could infer that the reaction corresponding to the first row has the reactants of  $x_2, x_4$  since they have negative weights, i.e., being consumed. The product is  $x_5$ , since it has a positive weight, i.e., being produced. Species of  $x_1, x_3$  do not participate in this reaction since they are neither consumed or produced by this reaction. For instance, we can infer the reaction formula of  $x_2 + x_4 \rightarrow x_5$ , which is the last reaction in (Eq. 9). The reaction orders in the first row of the heatmap for input weights are consistent with the stoichiometric coefficients. The rate constant of this learned reaction is 0.300 from the heatmap in the middle and is consistent with (Eq. 9). Similarly, the other three reaction formulas and rate constants are also accurately learned.

It is worth mentioning that the learned stoichiometric coefficients and reaction orders are very close to integers, although we did not apply any regularization to force them to be close to integers. This makes the approach suitable for learning elemental reactions, in which the stoichiometric coefficients and reaction orders are usually assumed to be an integer. In addition,



the stoichiometric coefficients and reaction orders for species not participated are learned to be very close to zero, although we did not apply any regularization to force them. It could be attributed to the regularization from the data itself and network structure.

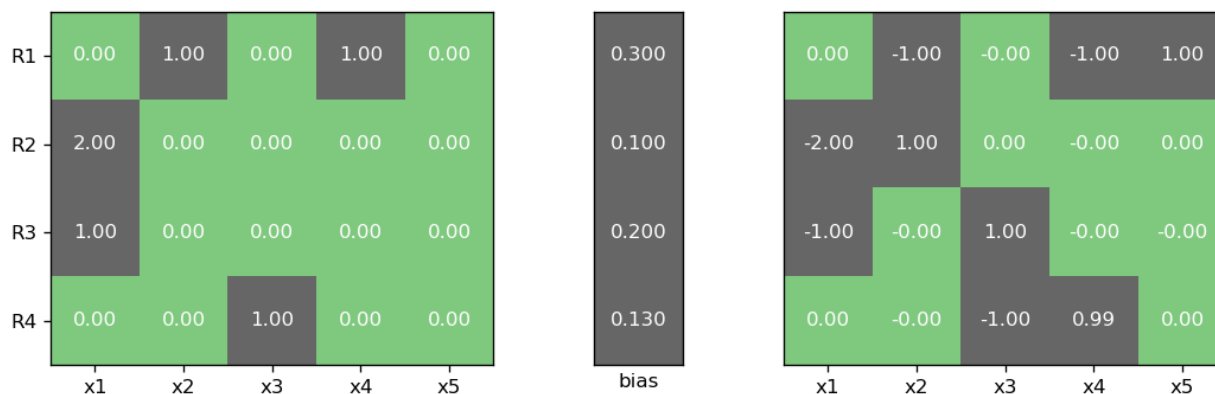


Fig. 6. The weights and bias of the trained CRNN with 4 hidden nodes. Left: weights of the input layer corresponding to reaction orders, middle: bias of input layer in exponential scale corresponding to rate constants, right: weights of the output layer corresponding to stoichiometric coefficients. Each row corresponds to a reaction.

We then demonstrate the  $L_1+L_2$  regularization approach. The number of hidden nodes is proposed to be 8, the hyperparameter  $\alpha$  for regularization in (Eq. 8) is set to be  $1e-8$ , and the CRNN is trained 100,000 epochs. The weights and bias of the trained CRNN are then shown in Fig. 7. Thanks to the regularization, only four of the learned reactions have large rate constants, and the rate constants for the rest of the unimportant reaction pathways are close to zero. For the active reaction nodes, the learned weights and bias are almost the same as Fig. 6. For the inactive nodes, the weights could be arbitrary. For instance, we can still discover a compact set of reaction pathways with  $L_1+L_2$  regularization even if we initially try a large number of hidden nodes.

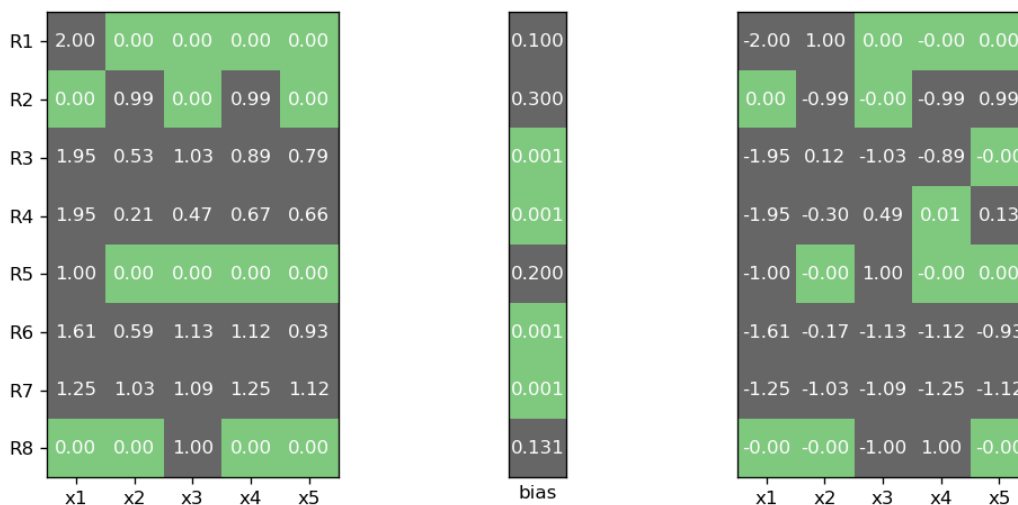


Fig. 7. The weights and bias of the trained CRNN with 8 hidden nodes. Left: weights of the input layer corresponding to reaction orders, middle: bias of input layer in exponential scale corresponding to rate constants, right: weights of the output layer corresponding to stoichiometric coefficients. Each row corresponds to a reaction.

### 3.2 Bio-diesel production with temperature dependence

The second case is to demonstrate the capability of learning the temperature dependence of the rate constants, i.e., the Arrhenius parameters in (Eq. 4). The reaction system, studied in (6, 33), is for biodiesel production via the transesterification of large, branched triglyceride (TG) molecules into smaller, straight-chain molecules of methyl esters. Darnoko and Cheryan (33) described three consecutive reactions, see (Eq. 10), which produce three byproducts, namely, diglyceride (DG), mono-glyceride (MG) and glycerol (GL). The pre-factor  $A$  in the logarithmic scale for three reactions are [18.60, 19.13, 7.93], and the activation energy is [14.54, 14.42, 6.47] kcal/mol. The initial reactants are TG and ROH. A total of 300 experiments are simulated in which the initial concentrations are randomly drawn from  $[TG] \in [0, 1]$ ,  $[ROH] \in [0, 1]$ , and the temperature is randomly drawn from  $T \in [50, 70]$  °C. In each case, the species concentrations and their temporal derivative were sampled every 2 time unit from 0 to 200 time units. Then totally, 30000 data pair is generated. In addition to the concentration of six species, the temperature,  $-1/RT$ , is also included as an input feature, according to (Eq. 4).

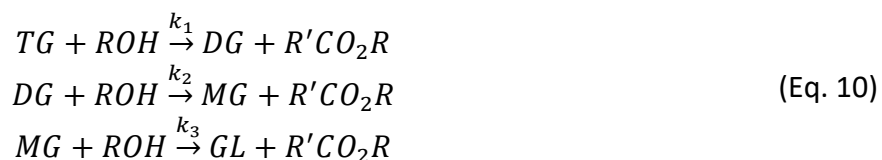


Figure 8 then shows the weights and bias of the trained CRNN with three hidden nodes. The reaction formula inferred from the output layer in the right heatmap is almost the same to (Eq. 10). The pre-factor  $A$  and activation energy  $E_a$  can be inferred from the bias and the last column of the input layer weights, and they are also very close to the underlying truth values. The reaction orders from the input layer in the left heatmap are also accurately recovered. Therefore, the CRNN approach is able to learn temperature-dependent reaction pathways that happen in food spoilage and energy conversion.

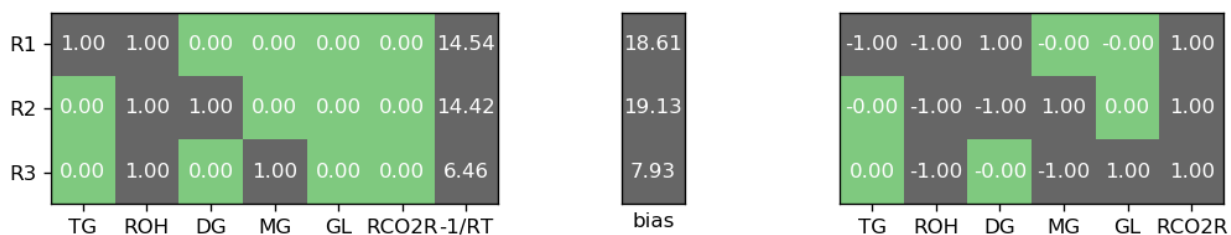
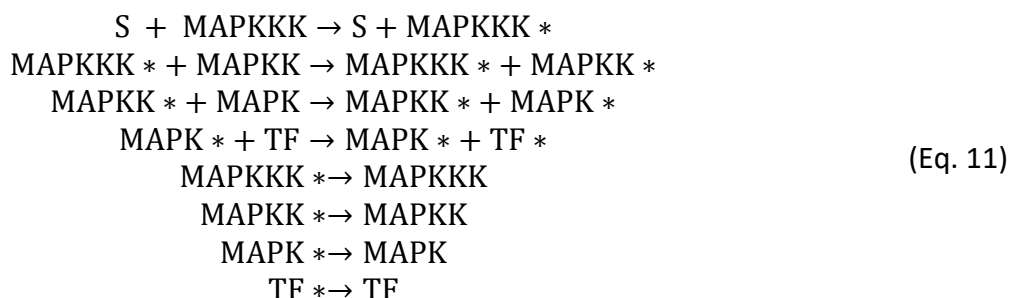


Fig. 8. The weights and bias of the trained CRNN with 3 hidden nodes for biodiesel production. Left: weights of the input layer corresponding to reaction orders and activation energies, middle: bias of input layer in exponential scale corresponding to pre-factor  $A$  of rate constants, right: weights of the output layer corresponding to stoichiometric coefficients. Each row corresponds to a reaction.

### 3.3 MAPK as a biochemistry catalysis reaction network

The third case is to demonstrate the learning of catalysis reactions in which catalyst presents in both reactants and products. Therefore, the binding between reaction orders and stoichiometric coefficients applied in 3.1 and 3.2 are relaxed in this case. The CRN considered is the mitogen-activated protein kinases (MAPK) pathway, taken from the work of Hoffmann et al. (11), which is an important regulatory mechanism of biological cells to respond to stimuli and is widely involved in proliferation, differentiation, inflammation, and apoptosis. The MAPK pathway consists of multiple stages of kinases that are either inactive or active, denoted by “\*”. The activation occurs due to phosphorylation catalyzed by the upstream kinase of the previous stage, and dephosphorylation is catalyzed by phosphatases. When the kinase is active, it can activate other downstream kinases of the next stage. Following (11), the MAPK pathway is modeled with three stages of kinases MAPK, MAPKK, and MAPKKK. The initial stimulus is called S, and the final substrate to be activated as a transcription factor TF. The ground truth reaction network consists of activation/phosphorylation and deactivation/dephosphorylation reactions, shown in (Eq. 11). All of the reaction rate constants are assigned to be 1.0.



A total of 300 experiments are simulated in which the initial concentrations randomly are drawn from  $[S] \in [0.001, 1]$ ,  $[\text{MAPKKK}] \in [0.1, 1]$ ,  $[\text{MAPKK}] \in [0.1, 1]$ ,  $[\text{MAPK}] \in [0.1, 1]$ ,  $[\text{TF}] \in [0.1, 1]$ . In each case, the species concentrations and their temporal derivative were sampled every 0.2 time unit from 0 to 10 time units. Then totally, 4500 data pair is generated.

Figure 9 then shows the weights and bias of the trained CRNN with eight hidden nodes. Since the catalyst presents both reactants and products. They are neither consumed nor produced. The weights in the output layer itself can not reveal the reaction formula. Instead, the reaction order inferred from the input weights could reveal the participation of the catalyst, i.e., the catalyst shows a positive reaction order but have a ‘zero’ stoichiometric in the output layer. For example, the first row in the left heatmap infers that the MAPK\* presents in the reactants, while the right heatmap infers a stoichiometric coefficient of zero for MAPK\*. Therefore, it is inferred that MAPK\* presents in both reactants and products as a catalyst. The rate constants in Fig. 9 are also very close to the assigned rates. The success CRNN approach in MAPK shall open the possibility of using CRNN to inference various catalysis reaction systems.

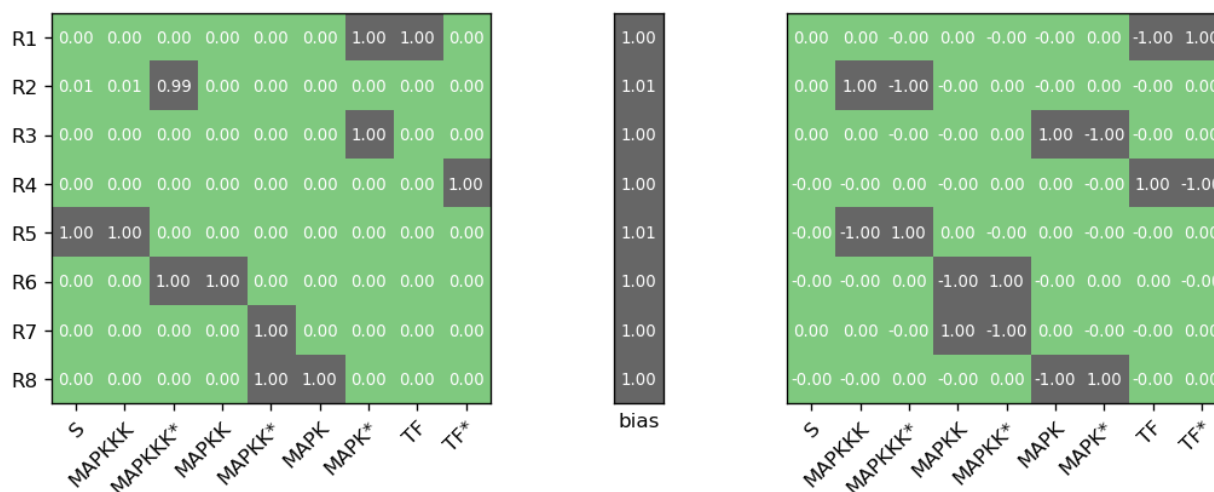


Fig. 9. The weights and bias of the trained CRNN with 8 hidden nodes for MAPK pathways. Left: weights of the input layer corresponding to reaction orders, middle: bias of input layer in exponential scale corresponding to rate constants, right: weights of the output layer corresponding to stoichiometric coefficients. Each row corresponds to a reaction.

## 4 Summary

This work presents a Chemical Reaction Neural Network (CRNN) approach for autonomous discovery of unknown reaction pathways from concentration time series data. The CRNN is equivalent to classical chemical reaction network, and it is formulated based on the fundamental physics laws of Law of Mass Action and Arrhenius Law. The reaction pathways and rate constants can be interpreted from the weights and bias of the CRNN. Stochastic gradient descent is adopted to optimize the large-scale non-linear CRNN models. The approach is demonstrated in three typical chemical systems from chemical engineering and biochemistry. Both the reaction pathways and the rate constants can be accurately learned. Those demonstrations shall open the possibility of discovering a large number of hidden reaction pathways in life science, environment, and engineering, including but not limited to gene expressions, disease progression, virus spreading, material synthesis and energy conversion.

## 5 Acknowledgment

SD would like to acknowledge the support from the d'Arbello Career Development allowance at Massachusetts Institute of Technology.

## 6 Reference

1. G. Pearson, *et al.*, Mitogen-Activated Protein (MAP) Kinase Pathways: Regulation and Physiological Functions\*. *Endocr. Rev.* **22**, 153–183 (2001).
2. C. K. Law, *Combustion physics* (Cambridge University Press, 2006).
3. H. N. Najm, B. J. Debuschere, Y. M. Marzouk, S. Widmer, O. P. le Maître, Uncertainty

- quantification in chemical systems. *Int. J. Numer. Methods Eng.* **80**, 789–814 (2009).
4. D. A. Sheen, H. Wang, The method of uncertainty quantification and minimization using polynomial chaos expansions. *Combust. Flame* **158**, 2358–2374 (2011).
  5. L. Cai, H. Pitsch, Optimized chemical mechanism for combustion of gasoline surrogate fuels. *Combust. Flame* **162**, 1623–1637 (2015).
  6. S. C. Burnham, D. P. Searson, M. J. Willis, A. R. Wright, Inference of chemical reaction networks. *Chem. Eng. Sci.* **63**, 862–873 (2008).
  7. T. R. Xu, *et al.*, Inferring signaling pathway topologies from multiple perturbation measurements of specific biochemical species. *Sci. Signal.* **3**, ra20–ra20 (2010).
  8. D. Langary, Z. Nikoloski, Inference of chemical reaction networks based on concentration profiles using an optimization framework. *Chaos* **29** (2019).
  9. N. Galagali, Y. M. Marzouk, Bayesian inference of chemical kinetic models from proposed reactions. *Chem. Eng. Sci.* **123**, 170–190 (2015).
  10. N. Galagali, Y. M. Marzouk, Exploiting network topology for large-scale inference of nonlinear reaction models. *J. R. Soc. Interface* **16**, 20180766 (2019).
  11. M. Hoffmann, C. Fröhner, F. Noé, Reactive SINDy: Discovering governing reactions from concentration data. *J. Chem. Phys.* **150**, 241723 (2019).
  12. N. M. Mangan, S. L. Brunton, J. L. Proctor, J. N. Kutz, Inferring Biological Networks by Sparse Identification of Nonlinear Dynamics. *IEEE Trans. Mol. Biol. Multi-Scale Commun.* **2**, 52–63 (2016).
  13. C. W. Gao, J. W. Allen, W. H. Green, R. H. West, Reaction Mechanism Generator: Automatic construction of chemical kinetic mechanisms. *Comput. Phys. Commun.* **203**, 212–225 (2016).
  14. C. Li, *et al.*, BioModels Database: An enhanced, curated and annotated resource for published quantitative kinetic models. *BMC Syst. Biol.* **4**, 92 (2010).
  15. F. Fröhlich, B. Kaltenbacher, F. J. Theis, J. Hasenauer, Scalable Parameter Estimation for Genome-Scale Biochemical Reaction Networks. *PLoS Comput. Biol.* **13** (2017).
  16. T. Lu, C. K. Law, Toward accommodating realistic fuel chemistry in large-scale computations. *Prog. Energy Combust. Sci.* **35**, 192–215 (2009).
  17. M. A. Savageau, Biochemical systems analysis. I. Some mathematical properties of the rate law for the component enzymatic reactions. *J. Theor. Biol.* **25**, 365–369 (1969).
  18. M. A. Savageau, Introduction to S-systems and the underlying power-law formalism. *Math. Comput. Model.* **11**, 546–551 (1988).
  19. E. O. Voit, R. G. Knapp, Derivation of the linear-logistic model and Cox’s proportional hazard model from a canonical system description. *Stat. Med.* **16**, 1705–1729 (1997).
  20. E. O. Voit, J. Almeida, Decoupling dynamical systems for pathway identification from metabolic profiles. *Bioinformatics* **20**, 1670–1681 (2004).
  21. K. O. Johansson, M. P. Head-Gordon, P. E. Schrader, K. R. Wilson, H. A. Michelsen, Resonance-stabilized hydrocarbon-radical chain reactions may explain soot inception and growth. *Science (80-. )*. **361**, 997–1000 (2018).
  22. I. Goodfellow, Y. Bengio, A. Courville, *Deep learning* (MIT press, 2016).
  23. M. Abadi, *et al.*, TensorFlow: Large-scale machine learning on heterogeneous systems, 2015. *Softw. available from tensorflow.org* **1** (2015).
  24. A. Paszke, *et al.*, Automatic differentiation in PyTorch. *31st Conf. Neural Inf. Process.*

- Syst.*, 1–4 (2017).
25. H. J. Curran, P. Gaffuri, W. J. Pitz, C. K. Westbrook, A comprehensive modeling study of n-heptane oxidation. *Combust. Flame* **114**, 149–177 (1998).
  26. L. Lu, X. Meng, Z. Mao, G. E. Karniadakis, DeepXDE: A deep learning library for solving differential equations (2019) (February 16, 2020).
  27. R. Chartrand, Numerical Differentiation of Noisy, Nonsmooth Data. *ISRN Appl. Math.* **2011**, 1–11 (2011).
  28. I. Knowles, R. Renka, Methods for numerical differentiation of noisy data. *Electron. J. Differ. Equ.* **21**, 235–246 (2014).
  29. D. P. Kingma, J. Ba, Adam: A Method for Stochastic Optimization. *arXiv Prepr. arXiv1412.6980* (2014).
  30. S. L. Brunton, J. L. Proctor, J. N. Kutz, Discovering governing equations from data by sparse identification of nonlinear dynamical systems. *Proc. Natl. Acad. Sci.* **113**, 3932–3937 (2016).
  31. T. Lu, C. K. Law, A directed relation graph method for mechanism reduction. *Proc. Combust. Inst.* **30**, 1333–1341 (2005).
  32. D. P. Searson, M. J. Willis, A. Wright, “Reverse Engineering Chemical Reaction Networks from Time Series Data” in *Statistical Modelling of Molecular Descriptors in QSAR/QSPR*, (Wiley-VCH Verlag GmbH & Co. KGaA, 2012), pp. 327–348.
  33. D. Darnoko, M. Cheryan, Kinetics of palm oil transesterification in a batch reactor. *J. Am. Oil Chem. Soc.* **77**, 1263–1267 (2000).